Journal of the European Ceramic Society **19** (1999) 255–262

PII: S0955-2219(98)00189-7
0955-2219/98/$—see front matter

The Role of Residual Stresses in Layered Composites of Y–ZrO_2 and Al_2O_3

Henryk Tomaszewski,[a]* Jan Strzeszewski[b] and Wojciech Gębicki[b]

[a]Institute of Electronic Materials Technology, Wólczyñska 133, 01-919 Warsaw, Poland
[b]Institute of Physics, Warsaw University of Technology, Koszykowa 75, 00-662 Warsaw, Poland

(Received 6 March 1998; accepted 31 July 1998)

Abstract

Laminar composites, containing layers of Y–TZP and either Al_2O_3 or a mixture of Al_2O_3 and Y–ZrO_2 have been fabricated using a sequential centrifuging technique of water solutions containing suspended particles. Controlled crack growth experiments with notched beams of composites were done and showed the significant effect of barrier layer thickness and composition on crack propagation path during fracture. Distinct crack deflection in alumina layers was observed. The increase of crack deflection angle with the alumina layer thickness was also found. In the case of the barrier layer made of a mixture, crack deflection did not occur independently on layer thickness. The observed changes have been correlated with the radial distribution of residual stresses in barrier layers created during cooling of sintered composites from fabrication temperature. The stresses found were the result of the difference in the thermal expansion and sintering shrinkage of alumina and zirconia and the crystallographically anisotropic thermal expansion of the alumina. The residual stress distribution has been measured by piezo-spectroscopy based on the optical fluorescence of Cr^{+3} dopants in alumina. © *1998 Elsevier Science Limited. All rights reserved*

Keywords: composite, thermal expansion, toughness, ZrO_2, Al_2O_3.

1 Introduction

In cooling sintered polycrystalline ceramics from their fabrication temperature residual stresses are created as a result of the difference in thermal expansion between the phases present. The knowledge of the residual stresses is important for a number of reasons. One is that the stresses across grain boundaries can be sufficiently large that grain boundary microcracking can occur. The importance of this phenomenon has led to a large body of work analyzing the mechanics of microcracking.[1–5] A second, related, reason is that the local residual stress affects the path of a crack as it propagates through the microstructure and is believed by many to lead to R-curve behaviour.[6,7] In a result, crack deflection and the increase in toughness of ceramics can be observed.[8,9] The aim of this work was to investigate laminar composites containing layers of Y-ZrO_2 and either Al_2O_3 or a mixture of Al_2O_3 and Y–ZrO_2 fabricated by sequential centrifuging of aqueous particle suspensions. The source of distinct stresses found here were the difference in thermal expansion and shrinkage between zirconia and alumina and the crystallographically anisotropic thermal expansion of the Al_2O_3 phase. The distribution of compressive stresses in barrier layers of composites occured to be dependent on layer thickness and composition (alumina only or a mixture) and to be regarded as a factor responsible for observed toughness increase.

2 Experimental Procedure

Laminar composites of Y–TZP and Al_2O_3 with layers with thicknesses of 10 to 60 μm (equal for both type of materials) were fabricated by the sequential centrifuging (Z382 Hermle) of powder suspensions. Aqueous slurries containing 5 to 10 wt% zirconia powder ($ZrO_2 + 3{\cdot}4$ mol% Y_2O_3, 0·6 μm median particle size obtained from Unitec Ceramics) or alumina powder (AKP-53 type, 0·29 μm median particle size obtained from Sumitomo) were prepared by ultrasonicating the powders in deionized water at pH 4. Cast samples were dried, additionally isostatically pressed at

*To whom correspondence should be addressed. Fax: +48-22-834-9003; e-mail: tomasz_h@sp.itme.edu.pl

120 MPa and then sintered at 1600°C. The larger shrinkage of the Y–ZrO_2 during sintering caused that in some layered composites the mixed composition of 50 vol% Al_2O_3 and Y–ZrO_2 was used instead of a pure Al_2O_3 to minimize this mismatch (Table 1). Micrographs of composite samples with both types of barrier layers were shown in Fig. 1. The samples after sintering were cut and ground to the dimensions of 45×4×1·5 mm and one surface perpendicular to the layers was polished. The sharp notch in the center of the beams was prepared with two diamond saws: 0·200 and 0·025 mm (Fig. 2).

Table 1. Shrinkage of materials used for Y-ZrO_2/Al_2O_3 composite preparation in a sintering temperature

Material used	*Shrinkage after sintering in 1600°C (%)*
Y–ZrO_2	19·04
Al_2O_3	16·27
Mixture of 50 vol% Al_2O_3 and Y–ZrO_2	18·47

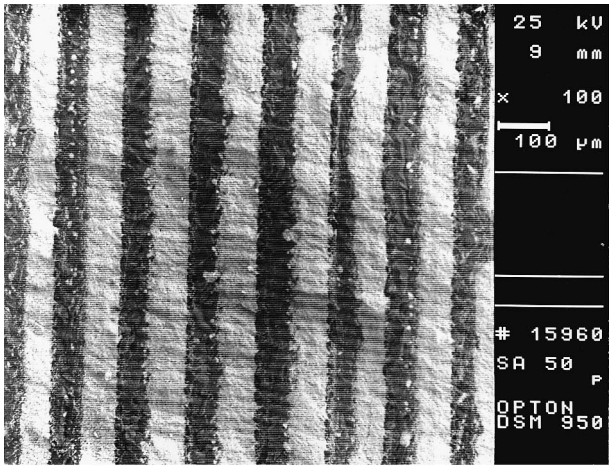

(a)

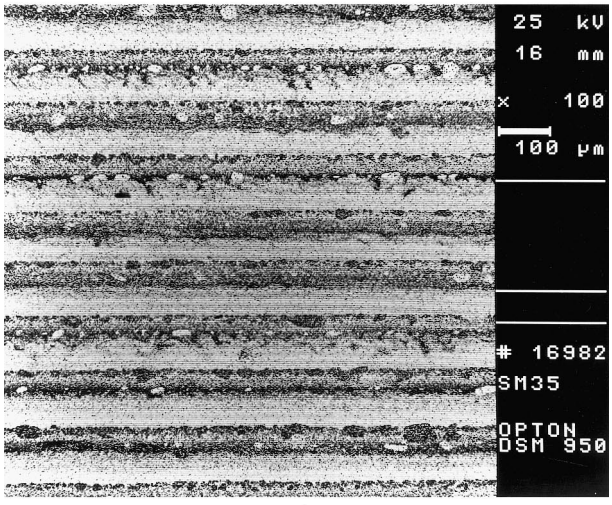

(b)

Fig. 1. Microstructure of layered composite with Y–TZP matrix and barrier layers (darker regions) consisted of (a) alumina and (b) a mixture of alumina and zirconia.

The tests of controlled crack growth were performed using Zwick machine of 1446 type. The notched beams were loaded in three-point bending with 1 μm/min loading speed and 40 mm bearing distance. The crack was initiated and slowly grown step by step in a controlled way by permanent loading and removing of the load. This procedure results in less than 100 μm increase of crack length by one step. The path of the crack during fracture of layered composite was registered by SEM using of OPTON DSM 950 microscope. All experiments were done at room temperature in normal air environments.

The spatial distribution of residual stresses within the alumina and a mixture of alumina and zirconia layer of the composites was measured using the piezospectroscopic technique. The method is based on the photostimulated fluorescence from trace Cr^{+3} ions in alumina.

The frequency shift $\Delta\nu$ of the two lines in the *R*-doublet is a measure of the elastic strain within the volume of material excited by the laser, following tensorial relation:[10]

$$\Delta\nu = \Pi_{ij}\sigma_{ij}$$

where: Π_{ij} are the piezospectroscopic coefficients and σ_{ij} are the stress components.

The piezospectroscopic measurements were made using an optical microscope with an attached spectrometer (DILOR X4800). An argon ion laser operating at wavelength of 514·5 nm was used as the excitation source. In each experiment a region of interest in the sample was first selected using the microscope then the laser beam was focused to a spot on that feature. This way the alumina or a mixture layer of composite were scanned by 5 to 10 μm steps. The intensities of the stimulated R_1 and R_2 fluorescence lines were typically collected by scanning the

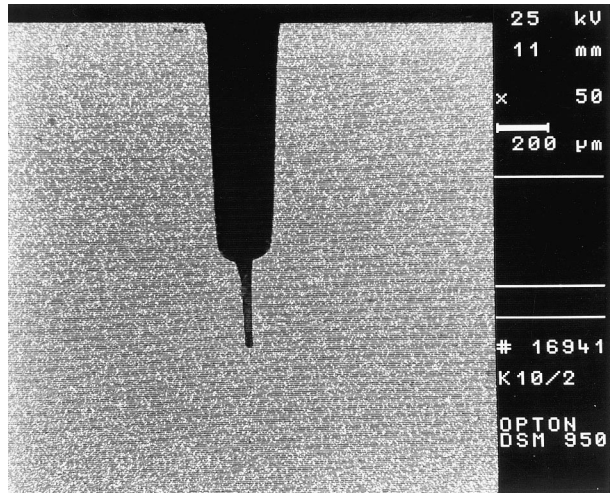

Fig. 2. An example of notched beam used in controlled crack propagation tests.

spectrometer gratings using steps of 0·2–0·4 wavenumbers and integrating over 0·5 s intervals. The collected data were subsequently analyzed with curve-fitting algorithms (double Lorentz function). The line position was identified by simultaneously fitting the R_1 and R_2 peaks using NiceFit software package. By using an objective lens of 100× magnifying power, a minimum spot size of $\sim 3\,\mu$m diameter could be achieved. It is known that both R_1 and R_2 lines shift to smaller wavenumber with increasing temperature, so a consistent calibration for the ruby was performed. Instrumental fluctuations were compensated by monitoring an external reproducible spectral line of a neon discharge lamp. Although the volume of material probed in the experiments was unknown, it was estimated that the spectroscopic information was obtained from a depth equalled spot size.

For determining the stresses in alumina, the R_1 line and piezospectroscopic coefficient (7·59 cm^{-1}/GPa), for hydrostatic stress state, found by He and Clarke[10] have been used.

The same method was used for calculating the residual stresses in alumina pellet prepared from the same type of alumina powder and at the same temperature of sintering. Although the average stress over the pellet must be zero, variations in stress from one grain to another being a result of the difference in thermal expansion coefficient along its *c*-axis ($\alpha_c = 9{\cdot}5 \times 10^{-6}{}^{\circ}C^{-1}$) and *a*-axis ($\alpha_a = 8{\cdot}6 \times 10^{-6}{}^{\circ}C^{-1}$) cause both a line shift and a broadening of the line due to superposition of spectra from individual fluorescing volumes. This way was possible to measure the everage value of the line shift and calculate subsequent everage value of local residual stresses in polycrystalline alumina.

The critical stress intensity factor, K_{Ic}, of composites was measured on notched beams described earlier by the method and relation proposed by Evans.[11]

3 Results and Discussion

Thermal expansion mismatch ($\alpha_{ZrO_2} = 12 \times 10^{-6}\,{}^{\circ}C^{-1}$, $\alpha_{Al_2O_3} = 9 \times 10^{-6}{}^{\circ}C^{-1}$) and shrinkage mismatch (see Table 1) between zirconia and alumina lead after cooling from fabrication temperature to residual stress distribution in layered composites shown at Fig. 3. In the layer with lower α and lower shrinkage, the biaxial compressive stress is expected and similarly, biaxial tensile stress in the layer with higher α and shrinkage. Such a distribution indicates that expected tensile stress in zirconia layer should promote opening the crack in the notched beam during bending. On the contrary,

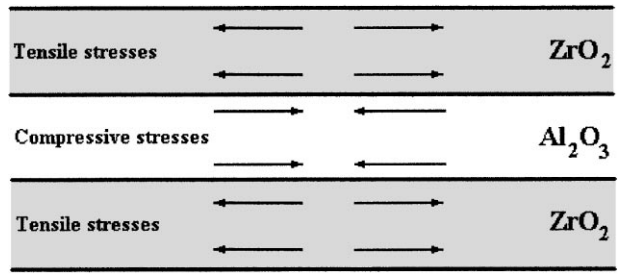

Fig. 3. Expected stress distribution in layered zirconia–alumina composites.

compressive stress in alumina layer will oppose the opening the crack. This expectation was confirmed by the tests of crack initiation in notched beams of composite studied. It occured that for the same layer thickness and bearing distance, 25% higher force had to be used to initiate the crack in the sample where notch ended at the beginning of alumina layer in comparison to the sample where it ended in zirconia layer. The character of the crack path during fracture was also different in these samples. In the case of second sample initiated crack propagated through zirconia layer perpendicularly to the layers.

In the case of first sample (notch ended at the begining of alumina layer), crack was deflected at the begining of its way through the alumina layer (see Fig. 4).

Further observation of controlled crack growth showed that deflection of crack takes place only in alumina layer. In zirconia layer the crack deflects back to its original direction. It was found that the magnitude of the crack deflection is dependent on alumina layer thickness of composite. The values of crack deflection angle (understood as a deflection angle from direction perpendicular to the layers) in a function of layer thickness are listed in Table 2. As can be seen, crack deflection angle increases with layer thickness. In 60 μm thick alumina layers crack deflects at 90° (Fig. 5). In layers with thickness of 10 μm and lower crack deflection does not take place (Fig. 6).

At the crack front, deflection process in alumina layers is more complicated than it was shown in Figs 5 and 6. Crack not only deflects but branches also (see Fig. 7) what distinctly enhances the length of the crack way and energy release during fracture through the alumina layer. After crack front moving farther, only one branch of the crack is widely opened but the rest of them is getting less visible for microscopic observations.

Described above crack behaviour was observed in the bulk of the material studied and it seems to be a result of residual stresses present in barrier layers. As can be seen from Figs 8–11, the frequency shift of the R_1 line and subsequent compressive stresses in

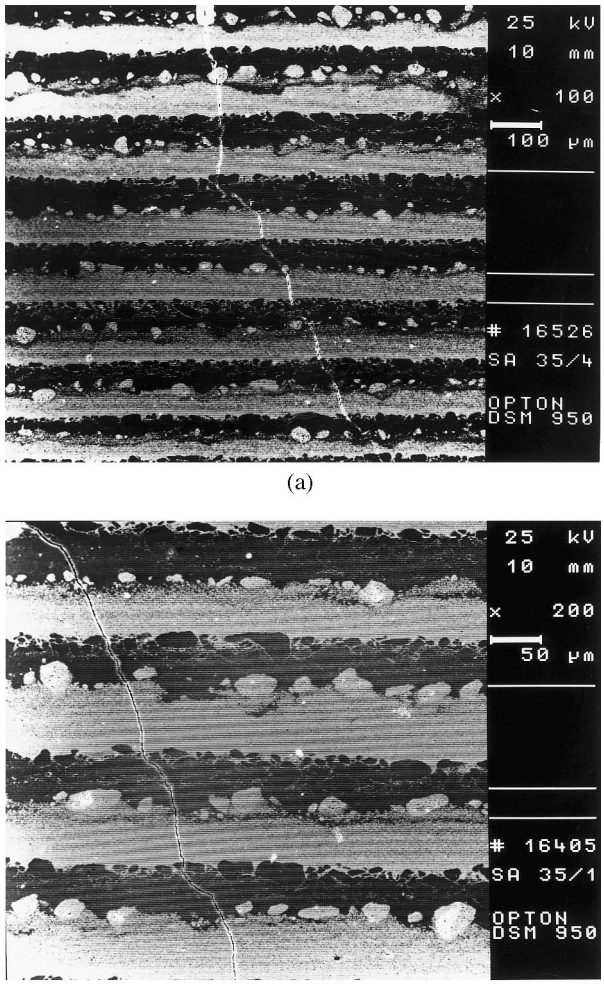

Fig. 4. Character of crack path during fracture of layered $Y–ZrO_2/Al_2O_3$ composite dependent on the type of layer where notch has been done: (a) the end of the notch in zirconia layer—*the crack propagates perpendicularly to the layer*, (b) the end of the notch in alumina layer—*the crack immediately deflects*.

Table 2. Mean value of crack deflection angle and gradient of compressive stresses in alumina layer of $Y–ZrO_2/Al_2O_3$ composite as a function of alumina layer thickness

Thickness of alumina layer (µm)	*10*	*25*	*40*	*60*
Mean value of crack deflection angle (°)	0	22 ± 5	62 ± 8	90
Gradient of compressive stresses, $\Delta\sigma$ (MPa)	13·2	50·8	158·1	188·4

alumina layers are not only a function of barrier layer thickness but a position across the layer also. Maximum of compressive stress equalled 280 MPa is observed at the interface and it is independent on alumina layer thickness. The minimum of stress is achieved in the center of the layer. However the stress in minimum is dependent on alumina layer thickness (see Table 2). In the case of 60 μm thick barrier layer the stress minimum equals 88·3 MPa. As it was said earlier, this value is exactly equal the residual stresses measured in alumina pellet prepared from the same

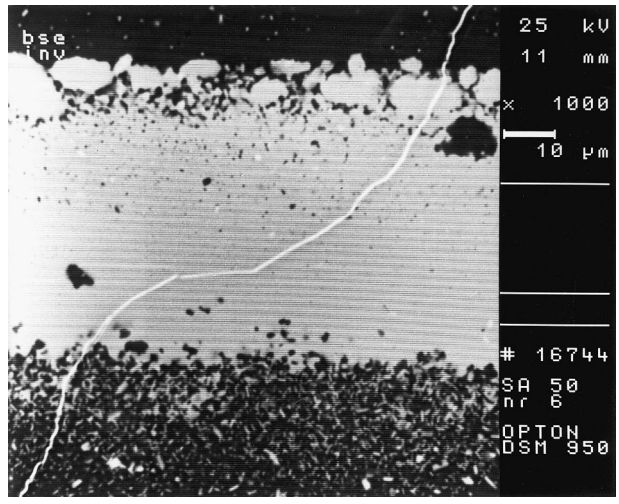

Fig. 5. The crack path in 55 μm thick alumina layer of $Y–ZrO_2/Al_2O_3$ composite (inverted image).

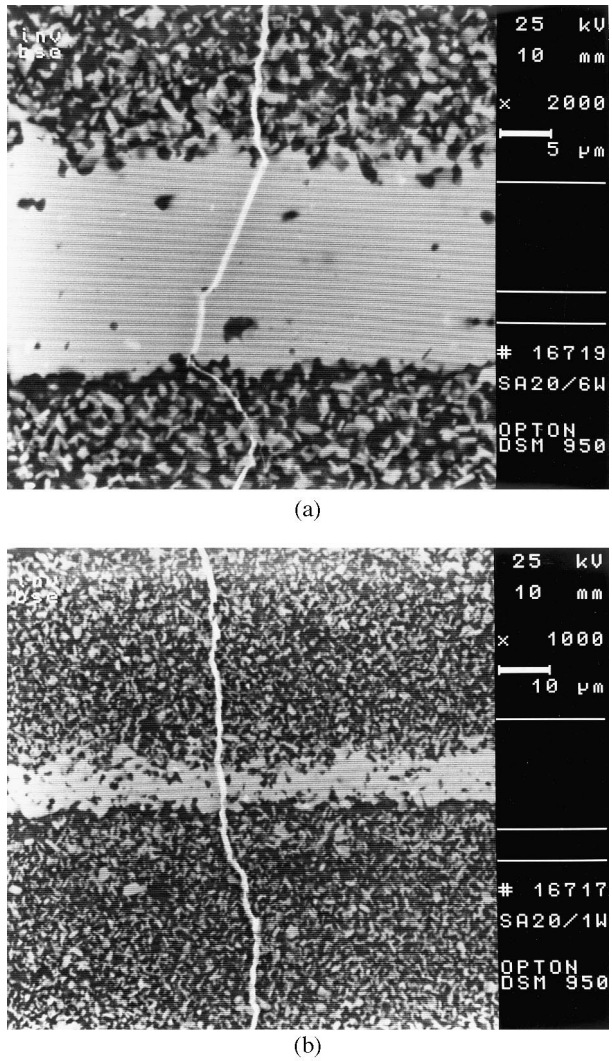

Fig. 6. The crack path in alumina layer of $Y–ZrO_2/Al_2O_3$ composite as a function of layer thickness: (a) 19·5 μm and (b) 8·2 μm (inverted image).

type of alumina powder and at the same temperature of sintering and caused by crystallographically anisotropic thermal expansion of the alumina only. It means also that the presence of compressive

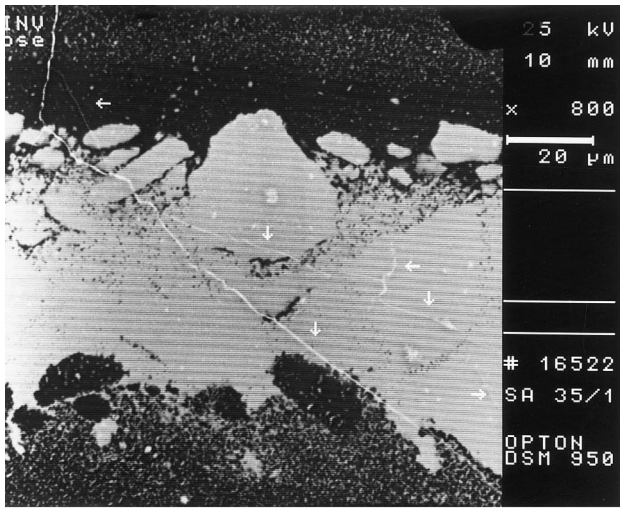

(a)

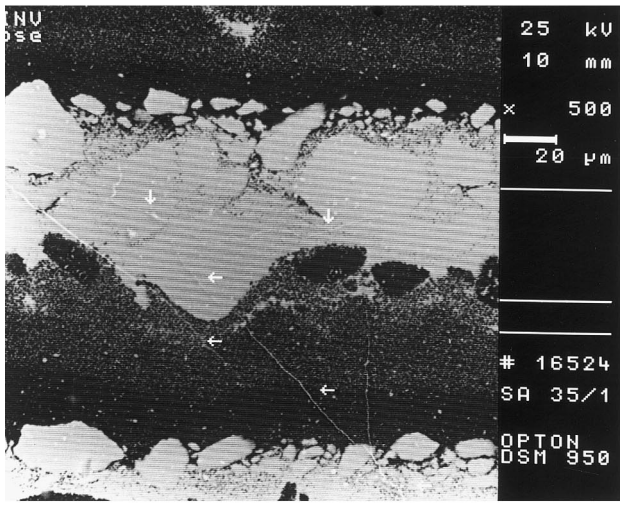

(b)

Fig. 7. The crack path in alumina layer of Y–ZrO_2/Al_2O_3 composite at the crack front (inverted image).

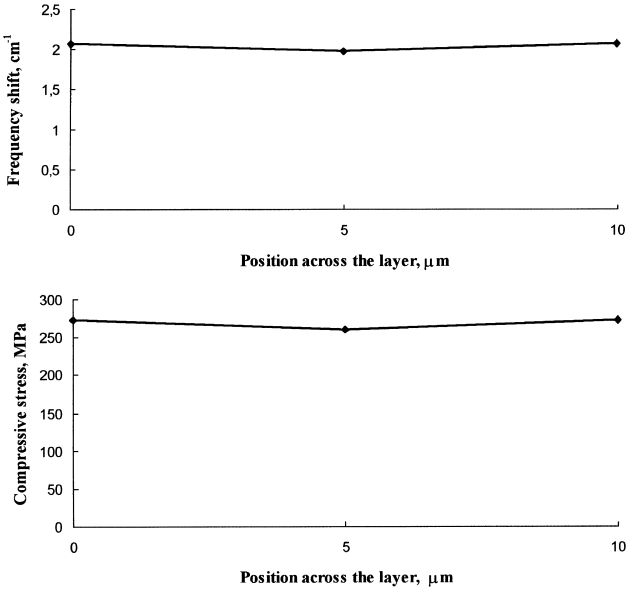

Fig. 8. Frequency shift of the R_1 line and compressive stresses in 10 μm thick alumina layer of Y–ZrO_2/Al_2O_3 composite as a function of position across the layer.

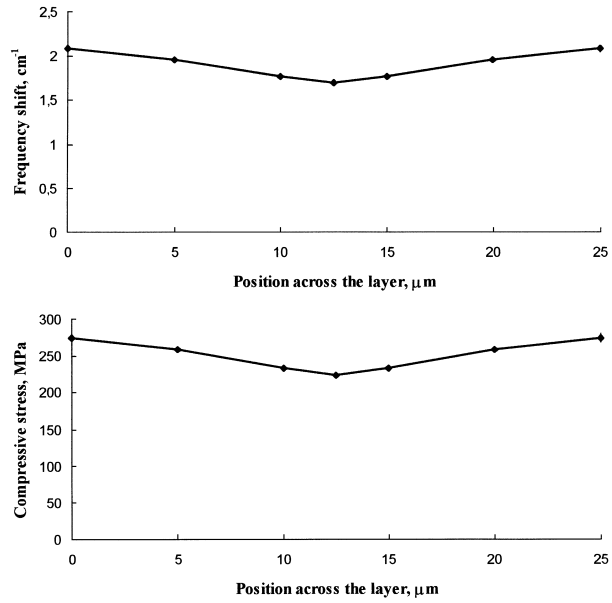

Fig. 9. Frequency shift of the R_1 line and compressive stresses in 25 μm thick alumina layer of Y–ZrO_2/Al_2O_3 composite as a function of position across the layer.

stress minimum in the center of thicker alumina layers can be the result of internal relaxation of stresses.

The compressive stress gradient (the difference of stress between the layer boundary and the center of the layer) listed in Table 2 can be correlated with the angles of crack deflection. Good correspondence indicates that the gradient can be regarded as an important factor responsible for the degree of crack deflection and further contribution of crack deflection mechanism in enhancing the toughness observed in layered composites (see Table 3).

To the stress distribution shown at Fig. 3 one new stress component should be added however. Finite element calculations[12,13] show that in layered materials not only biaxial stresses exist at the surface and far from the surface, but a stress perpendicular to the layer plane existing near the free surface that is highly localized, decreasing rapidly from the surface to become negligible at a distance approximately on the order of the layer thickness, also. This stress has a sign opposite to that of the biaxial stresses deep within the layer. Thus, when the biaxial stresses are compressive, there is a tensile stress perpendicular to the layer at and near the surface. This reversal of stresses was also observed by Cox[14] during his analysis of inclusions located either within a body or at the surface. Thus, a tensile stress field, localized near the surface, will be present in layers when the stress far from the surface is biaxial compressive. These tensile stresses can cause the extension of preexisting cracks. Such a cracks along the center of the two phase Al_2O_3/3Y–ZrO_2 layer (300 μm) bonded by two much thicker (3000 μm) 3Y–ZrO_2 layers

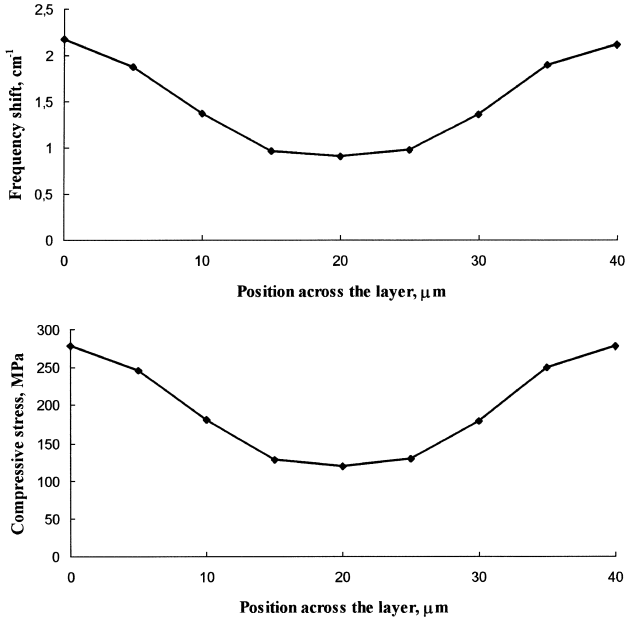

Fig. 10. Frequency shift of the R_1 line and compressive stresses in 40 μm thick alumina layer of Y–ZrO_2/Al_2O_3 composite as a function of position across the layer.

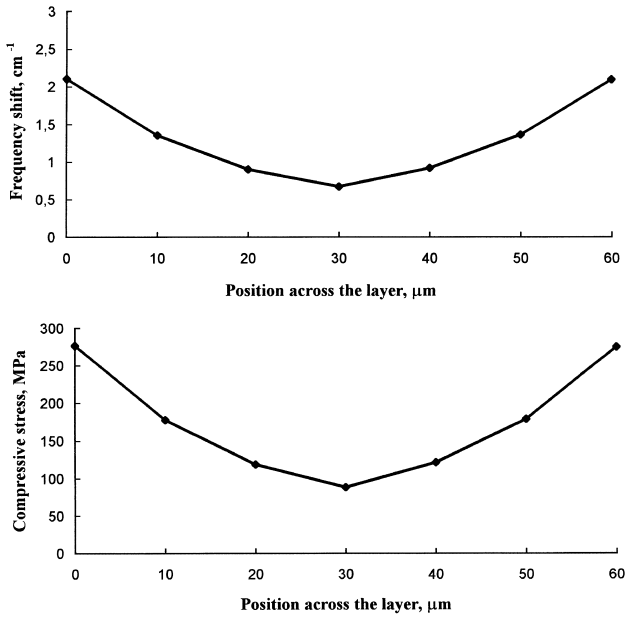

Fig. 11. Frequency shift of the R_1 line and compressive stresses in 60 μm thick alumina layer of Y–ZrO_2/Al_2O_3 composite as a function of position across the layer.

were observed after cooling from fabrication temperature by Ho *et al.*[15] and it was found that for a given residual stress, crack extension without any external stress will take place only when the layer thickness is greater than a critical value.

In our case matrix and barrier layer thickness was equal (10 to 60 μm) and cracks parallel to the layers were not found. But the presence of tensile stress perpendicular to the alumina layer plane with the maximum localized in the center of this

Table 3. Toughness of Y–ZrO_2/Al_2O_3 composite as a function of barrier layer thickness and composition

Composition of barrier layer	*Alumina*				*Mixture of alumina and zirconia*
Thickness of barrier layer (μm)	10	25	40	60	45
K_{Ic}, (MPa $m^{1/2}$)	7·20 ± 0·15	8·42 ± 0·55	9·99 ± 0·76	10·06 ± 0·33	7·11 ± 0·41

layer as was shown by FEM calculations[12,13] and confirmed by Ho *et al.*[15] seems to be helpful element in explanation of the role of compressive stress gradient in the crack deflection process observed in reported layered composites. The crack deflection in alumina barrier layers is a result of interaction of residual compressive stress acting in the plane parallel to the layers, and perpendicular to the layer and notch plane, tensile stress, both present in laminate after cooling from fabrication temperature and the third one, tensile applied stress in bending of notched beam. For a maximum of compressive stress gradient (the minimum of compressive stress) observed in the case of 60 μm thick alumina layer the tensile perpendicular stress begins to dominate and in a result the crack deflects in the center of the layer and propagates along the layer and then deflects back to the perpendicular direction when the compressive stress increases from the minimum in the center of the layer to the maximal value at the interface, as can be seen from Fig. 5. In the case of the thinnest alumina layer where the compressive stress across the layer becomes almost unchangable (the gradient is in minimum) the crack propagates through the layer without deflection.

The results obtained for composites with barrier layers made of an oxide mixture instead of a pure Al_2O_3 prepared to minimize the larger shrinkage of Y–ZrO_2 (see Table 1) are good confirmation of the thesis on the role of compressive stress gradient in observed crack deflection. Residual stresses in these layers should be present also, but their distribution seems to be different. It is expected they have rather local character—alumina grains in a mixture are stressed by zirconia grains and vice versa. Although perpendicular stress exists in this type of layers also, such a distribution of compressive stress should result in a lack of crack deflection. As it shown at Fig. 12, crack propagates through the barrier layer without deflection independently on layer thickness. The magnitude of frequency shift of the R_1 line and compressive stress in this case are slightly higher than in layers made of a pure alumina, but independent on position across the layer (Fig. 13).

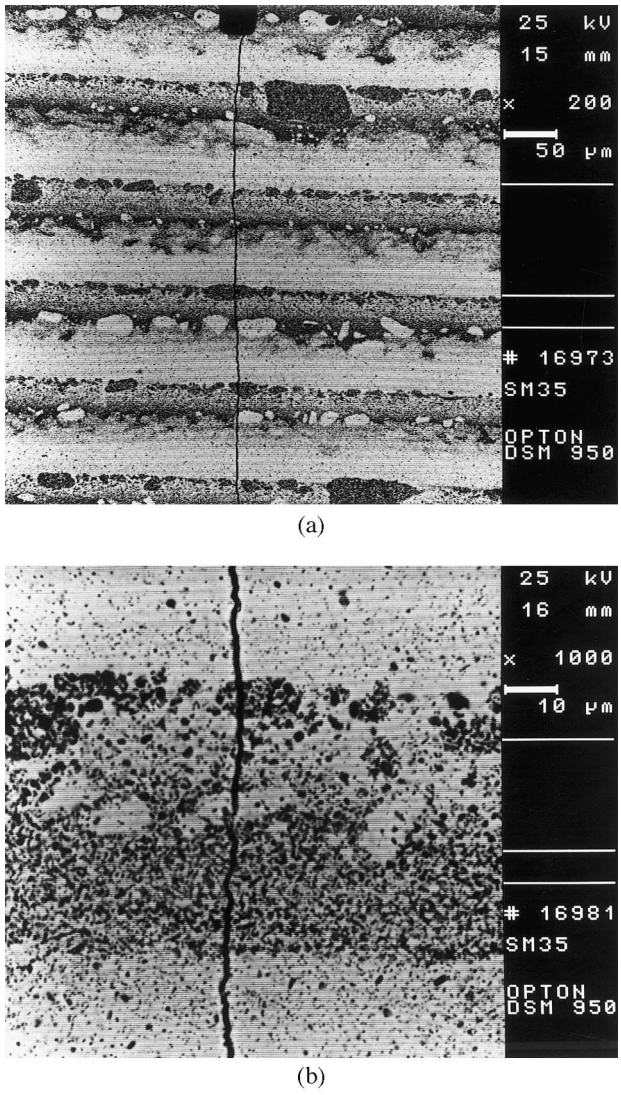

Fig. 12. The crack path during fracture of Y–ZrO_2/Al_2O_3 composite with barrier layers made of alumina and zirconia mixture.

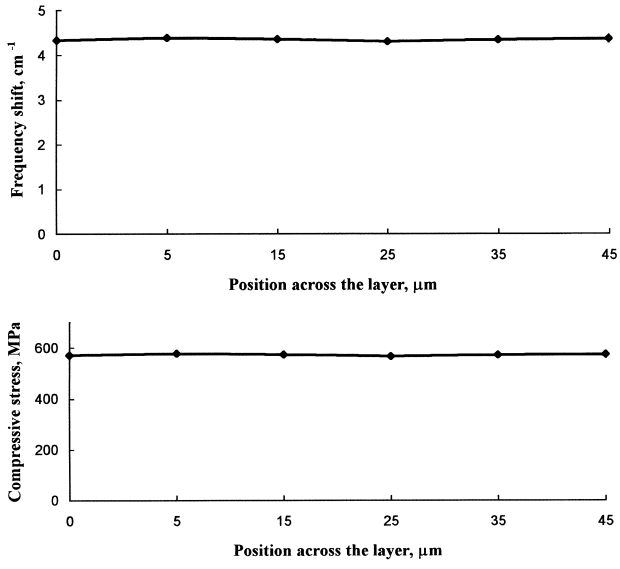

Fig. 13. Frequency shift of the R_1 line and compressive stresses in 45 μm thick barrier layer made of an oxide mixture of Y–ZrO_2/Al_2O_3 composite as a function of position across the layer.

4 Conclusions

The aim of this work was to determine the residual stress effect on character of crack propagation in layered ceramic composites prepared by sequential centrifuging of powder suspensions. During tests of controlled crack growth a distinct crack deflection in alumina layers was observed. As it occured the value of crack deflection angle was proportional to the layer thickness. In the case of layer thicknesses below 10 μm the crack was found to be undeflected. In barrier layers made of an oxide mixture crack deflection did not happen independently on layer thickness. This observations have been explained by measurements of residual stress distribution in barrier layers. The magnitude of compressive stress in alumina layer on the layer boundary was independent on layer thickness. However the layer thickness affected the gradient of stresses. The compressive stresses were found to decrease from the boundary of layer to the centre of alumina layer and here reached the minimum. The correlation between the value of crack deflection angle and the magnitude of stress gradient was observed. In the case of layer with thicknesses less than 10 μm, where crack did not deflect, the compressive stress gradient reached very small value. In the barrier layers made of an oxide mixture, higher compressive stresses were found. However the distribution and local character of these stresses resulted in the lack of crack deflection independently on layer thickness.

Elongation of crack way caused by crack deflection in alumina layer seemed to be responsible for observed enhancement in toughness of composites studied in a function of layer thickness.

Acknowledgements

This work was supported by Polish Committee for Scientific Research under grant No. 7S202 04607.

References

1. Clarke, F. J. P., Residual strain and fracture stress–grain size relationships in brittle solids. *Acta Metall.*, 1964, **12**(2), 139–143.
2. Evans, A. G., Microfracture from thermal expansion anisotropy. *Acta Metall.*, 1978, **26**(5), 1845–1853.
3. Clarke, D. R., Microfracture in brittle solids resulting from anisotropic shape changes. *Acta Metall.*, 1980, **28**(3), 913–924.
4. Tvegaard, V. and Hutchinson, J. W., Microcraking in ceramics induced by thermal expansion or elastic anisotropy. *J. Amer. Ceram. Soc.*, 1988, **71**(3), 157–166.
5. Ortiz, M. and Molinari, A., Microstructural residual stresses in ceramic materials. *J. Mech. Phys. Solids*, 1988, **36**(4), 385–400.
6. Cook, R. F., Fairbanks, C. J., Lawn, B. R. and Mai, Y.-W., Crack resistance by interfacial bridging: its role in determining strength characteristics. *J. Mater. Res.*, 1987, **2**(3), 345–356.

7. Svain, M. V., R-curve behaviour in a polycrystalline alumina material. *J. Mater. Sci. Lett*., 1986, **5**, 1393–1395.
8. Faber, K. T. and Evans, A. G., Crack deflection processes—I. Theory. *Acta Metall*., 1983, **31**(4), 565–576.
9. Faber, K. T. and Evans, A. G., Crack deflection processes—II. Experiment. *Acta Metall*., 1983, **31**(4), 577–584.
10. He, J. and Clarke, D. R., Determination of the piezospectroscopic coefficients for chromium-doped sapphire. *J. Amer. Ceram. Soc*., 1995, **78**(5), 1347–1354.
11. Evans, A. G., Fracture mechanics determination, In *Fracture Mechanics of Ceramics*, Vol. 1, ed. R. C. Bradt, D. P. H. Hasselman and F. F. Lange. Plenum Press, New York, 1974, pp. 17–48.
12. Harrison, N. L. and Harrison, W. J., The stresses in an adhesive layer. *J. Adhes*., 1972, **3**, 195–212.
13. Kirchner, H., Convay, J. and Segall, A. E., Effect of joint thickness and residual stresses on the properties of ceramic adhesive joints: I. Finite element analysis of stresses in joints. *J. Amer. Ceram. Soc*., 1987, **70**(2), 104–109.
14. Cox, B. N., Surface displacements and stress generated by a semi-elipsoidal surface inclusion. *J. Appl. Mech*., 1989, **56**, 564–570.
15. Ho, S., Hillman, C., Lange, F. F. and Suo, Z., Surface cracking in layers under biaxial, residual compressive stress. *J. Amer. Ceram. Soc*., 1995, **78**(9), 2353–2359.